



HAL
open science

Prevalence of Aseismic Slip Linking Fluid Injection to Natural and Anthropogenic Seismic Swarms

Philippe Danré, Louis de Barros, Frédéric Cappa, Jean-paul Ampuero

► **To cite this version:**

Philippe Danré, Louis de Barros, Frédéric Cappa, Jean-paul Ampuero. Prevalence of Aseismic Slip Linking Fluid Injection to Natural and Anthropogenic Seismic Swarms. *Journal of Geophysical Research: Solid Earth*, 2022, 127 (12), pp.e2022JB025571. 10.1029/2022jb025571 . hal-03936234

HAL Id: hal-03936234

<https://hal.science/hal-03936234>

Submitted on 12 Jan 2023

HAL is a multi-disciplinary open access archive for the deposit and dissemination of scientific research documents, whether they are published or not. The documents may come from teaching and research institutions in France or abroad, or from public or private research centers.

L'archive ouverte pluridisciplinaire **HAL**, est destinée au dépôt et à la diffusion de documents scientifiques de niveau recherche, publiés ou non, émanant des établissements d'enseignement et de recherche français ou étrangers, des laboratoires publics ou privés.

JGR Solid Earth

RESEARCH ARTICLE

10.1029/2022JB025571

Key Points:

- Scaling laws support that injection-induced and natural earthquake swarms have the same driving mechanism
- Aseismic slip is a key feature of earthquake swarms, although its contribution differs from one swarm to another
- We introduce a simple model based on fluid-induced aseismic slip propagation to relate observables to physical parameters

Supporting Information:

Supporting Information may be found in the online version of this article.

Correspondence to:

P. Danré,
danre@geoazur.unice.fr

Citation:

Danré, P., De Barros, L., Cappa, F., & Ampuero, J.-P. (2022). Prevalence of aseismic slip linking fluid injection to natural and anthropogenic seismic swarms. *Journal of Geophysical Research: Solid Earth*, 127, e2022JB025571. <https://doi.org/10.1029/2022JB025571>





Received 7 SEP 2022
Accepted 29 NOV 2022

Author Contributions:

Conceptualization: Philippe Danré
Investigation: Philippe Danré
Methodology: Philippe Danré, Louis De Barros, Frédéric Cappa, Jean-Paul Ampuero
Supervision: Louis De Barros, Frédéric Cappa, Jean-Paul Ampuero
Validation: Philippe Danré, Louis De Barros, Frédéric Cappa, Jean-Paul Ampuero
Visualization: Philippe Danré
Writing – original draft: Philippe Danré
Writing – review & editing: Philippe Danré, Louis De Barros, Frédéric Cappa, Jean-Paul Ampuero

© 2022. American Geophysical Union.
All Rights Reserved.

Prevalence of Aseismic Slip Linking Fluid Injection to Natural and Anthropogenic Seismic Swarms

Philippe Danré¹ , Louis De Barros¹ , Frédéric Cappa^{1,2} , and Jean-Paul Ampuero¹ 

¹Université Côte d'Azur, CNRS, Observatoire de la Côte d'Azur, IRD, Géoazur, Sophia Antipolis, France, ²Institut Universitaire de France, Paris, France

Abstract Anthropogenic fluid injections at depth induce seismicity which is generally organized as swarms, clustered in time and space, with moderate magnitudes. Earthquake swarms also occur in various geological contexts such as subduction zones, mountain ranges, volcanic, and geothermal areas. While some similarities between anthropogenic and natural swarms have already been observed, whether they are driven by the same mechanism, or by different factors, is still an open question. Fluid pressure diffusion or aseismic deformation processes are often proposed to explain observations of hypocenters migration during swarms, while recent models suggest that swarm seismicity is rather triggered by fluid-induced aseismic fault slip. Here, using a global compilation of 22 natural and anthropogenic swarms, we observe that duration, migration velocity, and total moment scale similarly for all swarms. This supports a common driving process for both natural and induced swarms. The scaling relations are similar to those found for slow slip events. These observations highlight the prevalence of fluid-induced aseismic slip as main driver of earthquakes migration during swarms. After quantifying aseismic slip released in the swarms, we propose an approach to estimate the seismic-to-total moment ratio, which we then compare to a theoretical estimation that depends on the migration velocity of the swarm and the effective stress drop. Our findings lead to a generic explanation of the process driving earthquake swarms that might open new possibilities to monitor seismic swarms.

Plain Language Summary Earthquake swarms are a particular type of seismic activity, during which a sequence of many earthquakes occurs without being initiated by a larger one. Swarms can be induced by anthropic hydraulic injections at depth, like during geothermal power exploitation and massive storage of diverse fluids (i.e., wastewater, CO₂) in porous reservoir formations. Natural earthquake swarms are also observed in a large variety of geological contexts. Previous works showed that natural and injection-induced swarms share some similarities, like the migration of seismicity. However, their underlying processes remain unclear. Here, we explain the observed similarities in both types of swarms by a model in which earthquakes are triggered by the propagation of an aseismic slip transient, which in turn is induced by pressurized fluid circulation. This model reconciles a suite of independent observations made over different length and time scales and provides a generic explanation of the driving process for the migration of earthquake swarms.

1. Introduction

Over the past 50 years, a number of studies have documented that fluid injection or extraction in subsurface reservoir formations can induce seismicity. These earthquakes can sometimes exceed magnitudes of 5 and have the potential to impact infrastructures and the public acceptance for geo-energy projects (Ellsworth, 2013; Keranen & Weingarten, 2018). The Rangely (US) experiment, conducted from 1969 to 1973, is one of the oldest and pioneering studies of seismicity caused by forced fluid injection (Raleigh et al., 1976). Another famous example is the 2006 Basel injection in Switzerland where 11,500 m³ of fluids were injected at about 5 km depth over the course of 6 days, leading to hundreds of earthquakes including an $M_L = 3.4$ event just a few hours after the shut-in of the injection well was decided (Deichmann & Giardini, 2009). More generally, anthropogenic hydraulic injections are responsible for many seismic sequences, in association with geothermal heat reservoir development (Albaric et al., 2014; Baisch et al., 2006; Charléty et al., 2007; Kwiątek et al., 2019), hydraulic fracturing (Schultz et al., 2018), wastewater storage (Keranen et al., 2013), CO₂ sequestration (Zoback & Gorelick, 2012), or, at a smaller scale, during controlled fault activation experiments (Guglielmi et al., 2015). Fluid-induced seismic activity is singular as it organizes as a swarm with earthquakes clustered in time and space with no distinguishable mainshock/aftershock pattern.

Interestingly, earthquake swarms are also found in nature in a diversity of geological contexts such as mountain ranges (Hatch et al., 2020; Jenatton et al., 2007; Ross & Cochran, 2021; Ruhl et al., 2016), rift zones (De Barros et al., 2020), subduction zones (Holtkamp & Brudzinski, 2011; Hoskins et al., 2021; Metois et al., 2016), along transform faults (Roland & McGuire, 2009), or in geothermal and volcanic areas (Hensch et al., 2008; Shelly et al., 2013). Fluids are thought to play a key role in natural swarms, either because seismicity is associated temporally or spatially with fluid circulation (Kraft et al., 2006; Montgomery-Brown et al., 2019; Shelly et al., 2013) or because they share similarities with injection-induced sequences (Skoumal et al., 2015). Indeed, the propagation of a seismicity front has been observed in sequences of anthropogenic origin (Goebel & Brodsky, 2018; Goebel et al., 2016) as well as in natural swarms (De Barros et al., 2020; Ross et al., 2020). Seismicity migration can be attributed to fluid pressure diffusion (Shapiro et al., 1997), aseismic slip (Roland & McGuire, 2009), or a combination of both (De Barros et al., 2021), as well as cascading events (Fischer & Hainzl, 2021). Studying the seismic moment released spatially during natural and injection-induced sequences also revealed a similar behavior (Fischer & Hainzl, 2017). However, despite those numerous observations, the drivers of seismicity in natural and induced swarms still need to be constrained.

To explain some of the observations made on numerous earthquake swarms, natural or injection-induced, fluid pressure diffusion has been routinely considered in the literature as the driver of seismicity. In this theory, the seismicity front migration would be a direct consequence of the propagation of an increase in fluid pressure, following a diffusive law, leading to a decrease in effective normal stress and associated fault strength, and therefore to seismic slip on asperities. The predicted shape of the migrating seismicity front in a distance–time diagram is a square root function, corresponding to the fluid pressure perturbation diffusion, with inferred diffusivities interpreted as hydraulic ones (X. Chen et al., 2012; Parotidis et al., 2004; Shapiro et al., 1997).

On the other hand, some swarms behave differently than a pressure diffusion process, suggesting another driving mechanism: they have high migration velocities, 2–3 orders of magnitude above usual observed values. It is the case for some swarms occurring on transform faults (Lohman & McGuire, 2007; Roland & McGuire, 2009) and in subduction areas (Vallee et al., 2013). This was confirmed in selected cases by the surface deformation recorded by geodetic measurements which shows that aseismic slip is the main mechanism driving seismicity (Hamiel et al., 2012; Hirose et al., 2014; Lohman & McGuire, 2007).

Recently, aseismic slip induced by fluid perturbations has been suggested to promote and drive seismicity in areas of hydrothermal circulation and anthropogenic fluid storage. During hydraulic stimulation experiments in subsurface reservoirs, aseismic slip was indeed proposed to favor seismicity by comparing fault deformations measured in boreholes and seismicity following a large-scale fluid injection test (Scotti & Cornet, 1994). Similarly, direct measurements of fault displacements and energy budget during in situ decimeter-scale injection tests (De Barros, Cappa, et al., 2019; Guglielmi et al., 2015) or during laboratory experiments (Goodfellow et al., 2015; Wang et al., 2020) showed an important aseismic component in the deformation compared to the seismic contribution. At a reservoir scale, geodetic studies revealed that in the Brawley Basin (California), fluid injection triggered aseismic slip which then led to an intense seismic swarm (Wei et al., 2015). A magnitude $M_w = 5.0$ slow slip event (SSE) was even directly induced by fluid injection during a hydraulic fracturing stimulation in the Rocky Mountains in Canada (Eyre et al., 2022). Indirectly, aseismic slip was also observed by studying repeating earthquakes during the Soultz-Sous-Forêt (France) sequences associated with geothermal stimulation (Bourouis & Bernard, 2007; Lengliné et al., 2014). More generally, at first order, seismic moment is expected to scale with the injected fluid volume (McGarr, 2014) for injection-induced sequences. However, discrepancies to this scaling have been systematically observed and can be reasonably explained by significant aseismic slip (De Barros, Cappa, et al., 2019; McGarr & Barbour, 2018).

These observations were then accompanied by a series of numerical modeling of injection-induced aseismic and seismic fault slip (Bhattacharya & Viesca, 2019; Cappa et al., 2019; Laroche et al., 2021; Wynants-Morel et al., 2020; Yang & Dunham, 2021; Zhu et al., 2020). Recently, hydromechanical modeling of fluid injection in a permeable slip-weakening fault showed that the increase of the critical earthquake nucleation size (the minimum size of a slip zone required for self-sustained seismic slip) with increasing fluid pressure leads to aseismic slip (Cappa et al., 2019). The fluid-induced aseismic slip may outpace the diffusing pressure front (Bhattacharya & Viesca, 2019; Laroche et al., 2021) and trigger seismicity near its edges where shear stresses increase (Wynants-Morel et al., 2020). In this case, the shear stress perturbation from aseismic slip is responsible for earthquake triggering and migration rather than fluid pressure diffusion (Wynants-Morel et al., 2020).

Weakening is not necessary: in strengthening faults, fluids can also induce a slow slip itself triggering seismicity (Dublanche & De Barros, 2021). Therefore, the seismic front migration maps the aseismic slip propagation. The front shape depends on fault criticality (De Barros et al., 2021) or on the injection parameters (Garagash, 2021; Saez et al., 2022), among other properties, leading to a diversity of migration shapes, some of which are not square root like.

At the same time, natural swarms are also accompanied by aseismic slip release, as revealed by geodesy and slip inversions (Gualandi et al., 2017; Hamiel et al., 2012; Jiang et al., 2022; Lohman & McGuire, 2007; Ruhl et al., 2016), or by studying velocity migrations and repeating earthquakes like during the 2015 swarm in the Gulf of Corinth, Greece (De Barros et al., 2020), or during a complex swarm in Nevada, USA (Hatch et al., 2020). The effective stress drop, defined for the full swarms by analogy with the stress drop for a single earthquake, is usually found to be low (0.01–1 MPa) for earthquake swarms (Fischer & Hainzl, 2017; Roland & McGuire, 2009), which is interpreted as indicative of aseismic deformation within the swarms. However, geodetic observations of aseismic slip associated with earthquake swarms remain rare and difficult to achieve, given their depth and low deformation rate. Thus, important questions on the contribution of aseismic slip during swarm activity remain.

All these observations, confirmed by numerical modeling and experiments, showed that earthquakes during fluid-induced seismic swarms may be only an indirect consequence of the fluid pressure perturbation. Indeed, the fluid pressure may primarily induce aseismic slip which, in turn, migrates and triggers the seismicity. In this study, we aim at exploring if such a model of fluid-induced aseismic slip as driving process of seismicity might be an adequate and plausible hypothesis to generally explain seismic swarms. Particularly, we aim at investigating if both injection-induced seismic sequences and natural swarms may be similarly explained by such a process.

To do so, we first explore the similarities between injection-induced and natural swarms in a global compilation of 22 cases. After presenting these seismicity catalogs, we measure their effective stress drops and migration properties. We then introduce a simple but realistic framework to estimate the aseismic slip released. The comparison across scales of swarm duration and migration velocity highlights the similarity between all types of swarms, which is also confirmed by the low effective stress drop and significant aseismic-to-seismic moment partitioning. Therefore, fluid-induced aseismic slip seems to explain most of the swarm features. Finally, we propose and validate a simple theoretical and physical model, based on observations, that explains both types of swarms.

2. Natural and Injection-Induced Catalogs

To explain the similarities between natural and injection-induced swarms, as well as their most remarkable features, we focus on a global data set of 22 earthquake swarms, from either injection-induced or natural origin. For natural earthquake sequences, we select swarms in which fluid processes have been previously discussed. For example, we do not consider the swarm studied by Lohman and McGuire (2007) which is interpreted as driven solely by a SSE. Likewise, we do not consider swarms taking place near volcanoes or in subduction zones as they might involve different processes (Roman & Cashman, 2006). For simplicity, the injection-induced sequences studied here are limited to sites where there is only one main injection well and to swarms that present a simple geometry. The earthquake catalogs used are described in detail in Texts S1 and S2 in Supporting Information S1, but we present them briefly below (Figure 1).

The eight natural swarms have diverse geological contexts. For instance, the 2003–2004 Ubaye (hereafter, named UBY) sequence (Jenatton et al., 2007) occurred in a near-zero strain-rate area in the southern French Alps, lasted ~2 years and comprised thousands of events (Daniel et al., 2011), while the 2014 Crevoux swarm lasted only 1 week and produced ~270 seismic events (De Barros, Baques, et al., 2019). The 2001 and 2015 Corinth (CRT) swarms (De Barros et al., 2020; Duverger et al., 2018) took place in a very fast extensional (~15 mm/year) rift zone in Greece with maximum magnitudes of $M_w = 3.8$ and $M_w = 2.5$, respectively. In California, an $M_w = 4.4$ earthquake occurred during the Cahuilla swarm (Ross et al., 2020), which lasted more than 4 years (CHA). Three swarms (SW2 in 2001, SW4 in 2008, and SW6 in 2013) along the Húsavík–Flatey fault system in Iceland are also considered in this study (Passarelli et al., 2018).

Most of the 14 injection-induced swarms we consider originate from geothermal exploitation. However, they span a wide range of characteristics, including the injected fluid volume and the injection depth. The Soultz-sous-Forêts (SZ) stimulations took place in 1993, 1995, 1996, 2000, 2003, and 2004 in Eastern France during a tenth of days, with injected volumes up to 37,000 m³ along several distinct wells, each time inducing a prolific

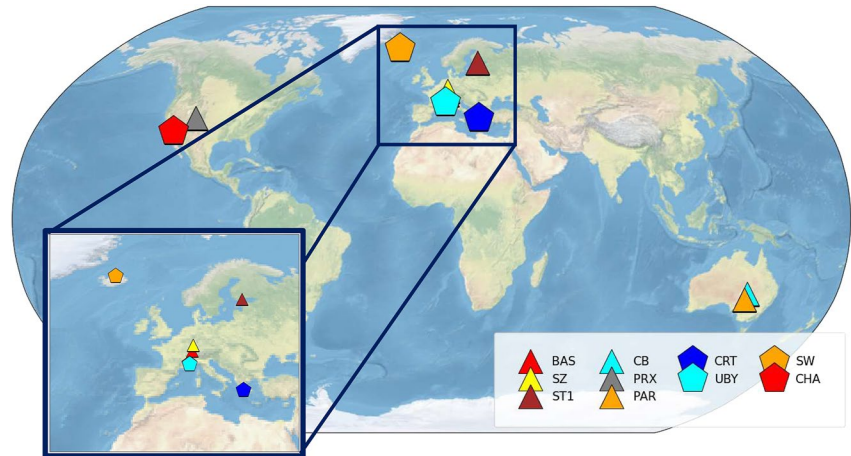


Figure 1. Location of studied seismic swarms. Pentagons indicate natural swarms while triangles indicate injection-induced ones. BAS, Basel; SZ, Soutz-sous-Forêts; CB, Cooper Basin; PRX, Paradox Valley; PAR, Paralana; CRT, Gulf of Corinth; UBY, Ubaye; CHA, Cahuilla.

seismic response with hundreds of events or more (Bourouis & Bernard, 2007; Calò & Dorbath, 2013; Cuenot et al., 2008; Dyer et al., 2004; Gerard et al., 1997). Just nearby, the Rittershoffen seismic sequences were induced also by a hydraulic stimulation (Lengline et al., 2017). The Paralana, Cooper Basin 2003 and 2012 injections (PAR, CB03, and CB12) took place in Australia and also exhibited an intense seismic activity associated with fluid injection (Albaric et al., 2014; Baisch et al., 2006, 2015). Recently, the ST1 sequence in Finland corresponds to a control experiment aiming at mitigating the seismicity induced by fluid injection. In this case, 18,000 m³ of fluids were injected during 49 days, leading to hundreds of events but successfully preventing the occurrence of earthquakes of magnitude greater than 2.0 (Kwiatek et al., 2019). Finally, the Paradox Valley swarm (PRX) is induced by wastewater disposal, with several millions cubic meters of fluids injected since 1985 leading to a long-lasting earthquake activity with several events of magnitudes $M_w > 4$ (Ake et al., 2005).

3. Methods

To analyze this global compilation of seismic swarms, we measure the migration velocity of their front and their effective stress drop. Assuming a migrating fluid-induced aseismic slip drives seismicity, we then estimate the total moment (seismic plus aseismic) by analogy with seismicity on fault asperities triggered by SSEs and relate it to a simple theoretical mechanical framework.

3.1. Migration Velocity

The average migration velocity of each swarm is estimated by fitting the seismicity front with a linear model. Seismicity fronts have been modeled by either a diffusive law, constant speed or more complex relations (De Barros et al., 2021; Goebel & Brodsky, 2018). However, here, the shape of the migration is not investigated, as we only focus on estimating an average migration velocity, in order to make first-order comparisons among swarms. The spatial origin of the swarm is chosen as the median of the hypocentral coordinates of the 10 first events. The origin time is defined as the time of the first event. We compute the seismicity front as the 90th percentile of event distances relative to the swarm origin in a sliding window containing 50 events (Figure 2). Migration duration is defined as the time during which the front distance increases continuously (see Table S3 in Supporting Information S1). We fit a linear model over the measured seismicity front during the migration period to get an average migration velocity for each sequence. Note that the obtained misfits (r^2 values) are similar when using a linear fit or a diffusive law (see Table S2 in Supporting Information S1), in part because of the scattering of the seismicity front data points. This implies that seismic front alone cannot help discriminating between driving processes. Additional description of the methods and migration fits for all swarms can be found in Text S3 and Figures S1 and S2 in Supporting Information S1.

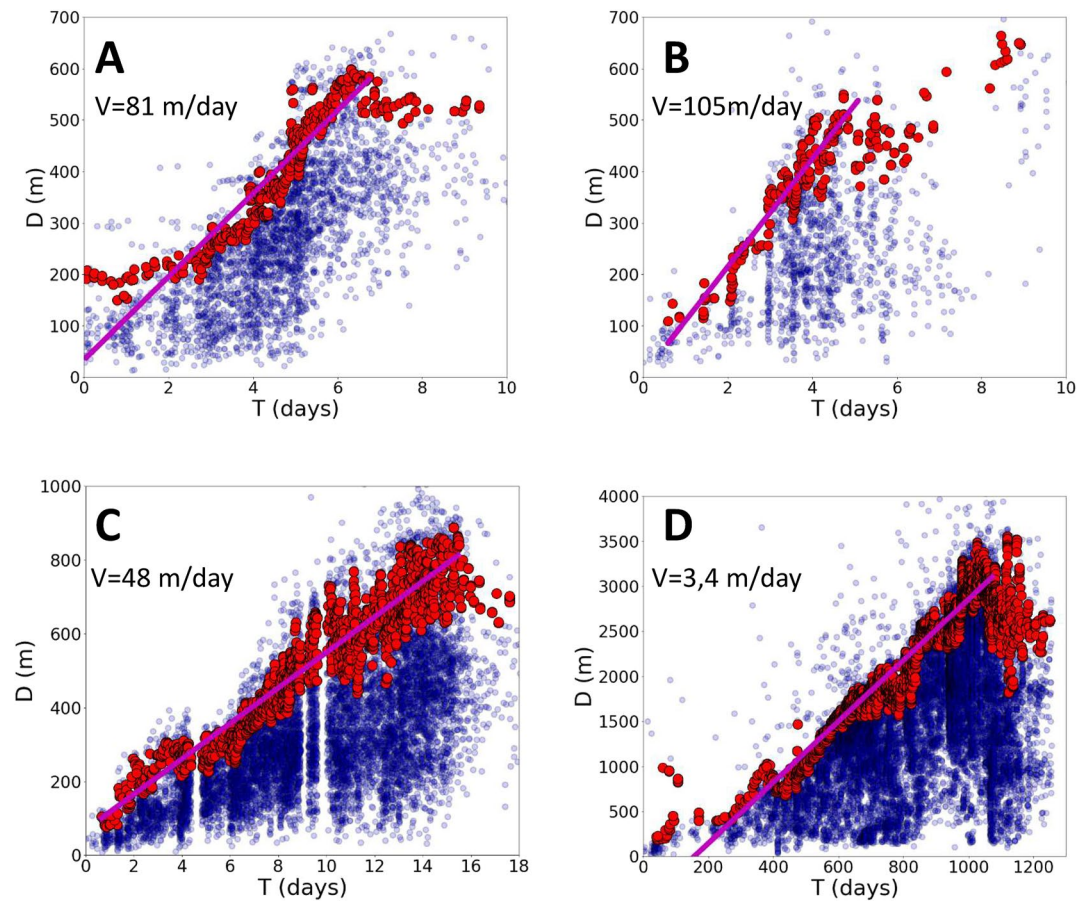


Figure 2. Distance–time plot of seismicity and average migration speed estimates for the (a) Basel, (b) Corinth, (c) Soultz-Sous-Forêts 1993, and (d) Cahuilla swarms. Blue points indicate the distance to the origin (m) and occurrence time (days) of each earthquake. Red circles correspond to the seismicity front. Magenta lines are the linear best fit made over the seismicity front during the migration period. For the other swarms, see Figures S1 and S2 in Supporting Information S1.

3.2. Effective Stress Drop

We selected swarms with simple spatial geometry, that can be assumed coplanar. This is quantified by the ratio of eigenvalues of the covariance matrix of their 3D coordinates (Michelini & Bolt, 1986, see Table S1 in Supporting Information S1). For the Parana sequence, despite more scattered hypocenters, we still consider seismicity to be coplanar given the high location uncertainties. Following the approach of Fischer and Hainzl (2017), the seismicity area is then computed by fitting a 2D plane over the 3D distribution of hypocenters after removing the few outliers in the catalogs outside the swarm area (see Text S4 in Supporting Information S1). Hypocenters are then projected over the plane and a convex hull is fitted to delineate and compute the seismicity area S . We then compute the radius of the seismicity area, assuming it is circular at first order, with $R = \sqrt{S/\pi}$.

By analogy with the moment–size relationship for circular ruptures, the effective stress drop of a swarm is defined as (Fischer & Hainzl, 2017)

$$\Delta\sigma_e = \frac{7M_{0,\text{seismic}}}{16R^3} \quad (1)$$

where $M_{0,\text{seismic}}$ is the cumulative seismic moment during the swarm. A low effective stress drop suggests seismic asperities are far apart, whereas values close to earthquake stress drops, typically around 1–100 MPa (Cocco et al., 2016), suggest that seismic asperities cover most of the slipping area. The former has been proposed to indicate a large contribution of aseismic slip during swarms (Fischer & Hainzl, 2017).

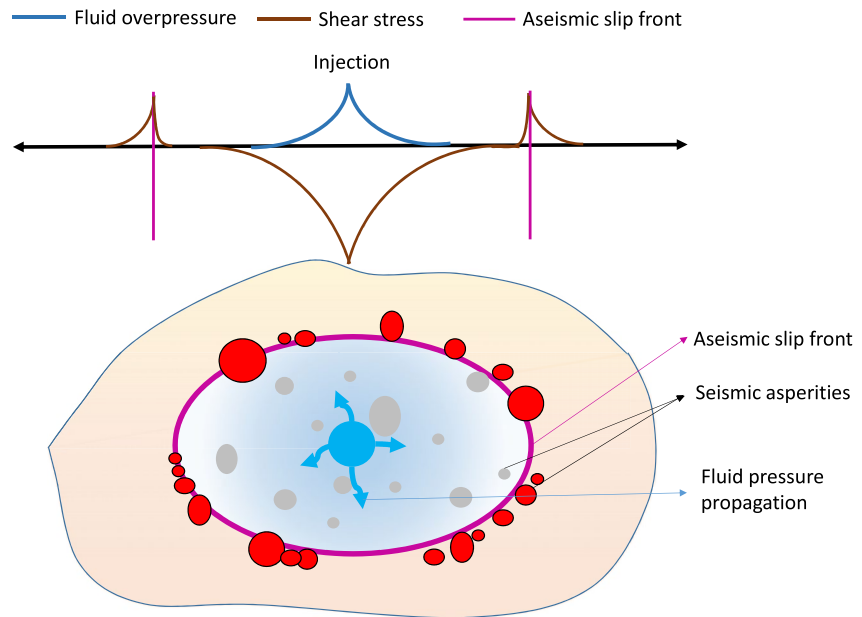


Figure 3. Schematic view of the model considered here, based on observations and hypothesis that depicts simplistically the processes occurring during swarm propagation. Aseismic slip front (purple) propagation leads to shear stress concentration at its tips (brown), triggering seismicity on asperities (red patches), which correspond to the seismicity front. Seismicity is also triggered within the slipping zone (gray patches).

3.3. Total Moment Estimation

The total moment is defined as the sum of the seismic and aseismic moments. Aseismic slip quantification is difficult for injection-induced sequences because the associated deformations are small and extend over long durations, leading to small strain rates that are hard to observe from the Earth surface. The same issue affects natural swarms, in addition to the instrumental limitations, the distance between sensors and the source depth. For instance, during the Icelandic swarms, despite the substantial aseismic slip expected, no corresponding signal was detected on the neighboring GPS stations (Passarelli et al., 2018).

We propose a simple way to estimate, roughly, the amount of aseismic slip in a swarm in the absence of geodetic data. Studies of slow slip transients in subduction zones and on creeping faults have shown that the cumulative slip of repeating earthquake sequences equals the surrounding aseismic slip (Matsuzawa et al., 2004; Uchida, 2019). Based on recent works demonstrating that the migration front of seismicity can be directly triggered by the shear stress perturbation induced by propagating aseismic slip initiated by fluid pressurization (Cappa et al., 2019; Wynants-Morel et al., 2020; Figure 3), we can assume an analogy with seismicity triggered by slow slip transients along faults. Therefore, we may suppose that the slip released seismically over discrete asperities equals the surrounding aseismic slip. We neglect the contribution of afterslip given that it may represent only $\sim 20\%$ of the slip occurring over the seismically slipping area for simulations of small repeating earthquakes (T. Chen & Lapusta, 2009). Assuming that the asperity associated with the largest earthquake in the swarm only ruptures once, its slip gives an order of magnitude estimate of the slip over the whole area. For each sequence, we consider the largest event, with moment $M_{0,\max} = GD_{\max}\pi R_{\max}^2$, assuming a circular rupture of radius R_{\max} , a shear modulus $G = 30$ GPa (a conventional value for crustal rocks) and static stress drop $\Delta\sigma_{\max} = 7M_{0,\max}/16R_{\max}^3$ (Madariaga, 1976) of 10 MPa (unless a more precise value is provided in the literature, see Text S2 in Supporting Information S1), and compute its slip D_{\max} as (Madariaga, 1976)

$$D_{\max} = M_{0,\max}^{1/3} \frac{(16\Delta\sigma_{\max})^{2/3}}{G\pi^{2/3}} \quad (2)$$

Given that seismic moment is released over discrete asperities and aseismic slip is released in between them, we estimate the total moment over the seismicity area as

$$M_{0,\text{total}} = GD_{\text{max}}S \quad (3)$$

We apply this approach to the Salton Trough sequence, which was interpreted to be solely driven by aseismic slip based on geodetic measurements (Lohman & McGuire, 2007). The total moment obtained with our method matches the value determined with geodesy: $M_w = 5.79$ and $M_w = 5.75$, respectively (see Text S5 in Supporting Information S1). The seismic moment is only 20% of the total moment (Lohman & McGuire, 2007).

While the effective stress drop qualitatively indicates the importance of aseismic slip during a swarm, the rough quantification approach proposed here allows us to better constrain the aseismic moment of each sequence.

3.4. Seismic-To-Total Moment Ratio

By considering that the total (seismic and aseismic) slip is equivalent to a single slip event over a circular area of radius R and stress drop $\Delta\sigma_{\text{total}}$ (Figure 3), we have (Madariaga, 1976)

$$M_{0,\text{total}} = \frac{16}{7} \Delta\sigma_{\text{total}} R^3 \quad (4)$$

The rupture velocity of a SSE is related to its stress drop and to its maximum slip velocity V_{max} by (Ampuero & Rubin, 2008; Passelègue et al., 2020; Rubin, 2008)

$$V_{\text{rupt}} = \frac{GV_{\text{max}}}{n\Delta\sigma_{\text{total}}} \quad (5)$$

where n is the ratio between the strength drop (peak minus residual frictional strength) and the stress drop, $\Delta\sigma_{\text{total}}$ (initial minus residual stress). In several numerical simulations of slow slip, $n \sim 10$ (Hawthorne & Rubin, 2013; Lambert et al., 2021).

We hypothesized that seismicity is triggered by fluid-induced aseismic slip. Therefore, the seismicity front follows the aseismic slip front (Bhattacharya & Viesca, 2019; De Barros et al., 2021; Wynants-Morel et al., 2020) like observed with tectonic tremors migration and slow slip propagation in subduction zones (Bartlow et al., 2011; Wech & Bartlow, 2014). The migration velocity of the swarms is then equal to the rupture velocity of the aseismic slip ($V_{\text{rupt}} = V_{\text{migr}}$). Our hypothesis based on the previously discussed observations is summarized in Figure 3. Combining Equations 4 and 5 we then have

$$M_{0,\text{total}} = \frac{16}{7} \frac{GV_{\text{max}}}{nV_{\text{migr}}} R^3 \quad (6)$$

This leads us to the following expression for the ratio r of seismic-to-total moment:

$$r = \frac{M_{0,\text{seismic}}}{M_{0,\text{total}}} = \frac{7M_{0,\text{seismic}}}{16R^3} \frac{nV_{\text{migr}}}{GV_{\text{max}}} \quad (7)$$

This equation can be written in a more compact form using the effective stress drop (Equation 1):

$$r = \frac{n\Delta\sigma_c V_{\text{migr}}}{GV_{\text{max}}} \quad (8)$$

This relation links the ratio of the cumulative seismic moment to total moment to the product of the migration velocity and the effective stress drop of the swarm.

4. Results

4.1. Aseismic Slip Transients Driving Natural and Induced Seismic Swarms

The estimated velocities of the 22 swarms studied here range from a few meters per day, like for the Cahuilla swarm (Ross et al., 2020), to more than 1 km/day, like for the Rittershoffen sequence (Lengline et al., 2017). Figure 4 shows the migration velocity (V) as a function of swarm duration (T), for induced and natural swarms (see also Table S3 in Supporting Information S1). We included velocity measurements from the literature for additional cases (Duboeuf, 2018; Duverger et al., 2015; Kim, 2013; Seeber et al., 2004; Yoshida & Hasegawa, 2018).

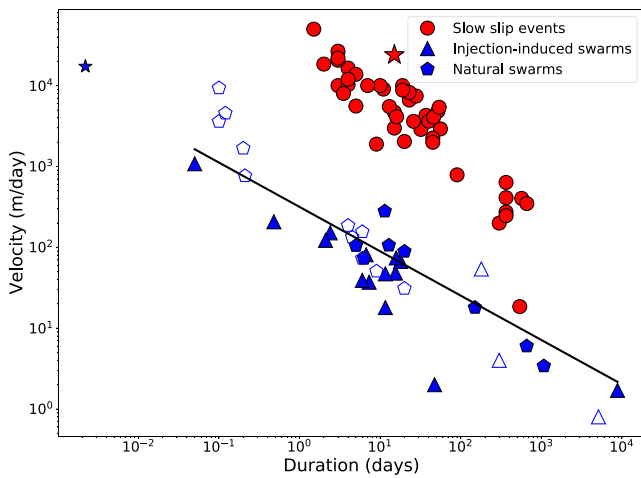


Figure 4. Scaling of migration velocity with duration for swarms and slow slip events (SSEs). Red dots represent SSE data from Gao et al. (2012). Filled triangles and pentagons represent injection-induced and natural swarms, respectively, for which we determined migration velocity and duration based on seismicity catalogs. Empty symbols represent migration velocities and durations directly taken from the literature (Duboeuf, 2018; Duverger et al., 2015; Kim, 2013; Seeber et al., 2004; Yoshida & Hasegawa, 2018). Red star represents the 2005 Salton Trough swarm (values from Lohman & McGuire, 2007) and blue star represents one value obtained from numerical modeling by Wynants-Morel et al. (2020). Black line represents the best fitting power law relation between velocities and durations of natural and induced swarms ($R^2 = 0.76$).

For the sake of comparison, we also show the migration velocity of SSEs in subduction zones (Gao et al., 2012). For these events, velocities correspond to the propagation of aseismic slip, which is characterized either with geodesy (Schmidt & Gao, 2010) or with tremor migration (Bartlow et al., 2011; Ito et al., 2007).

Two main observations can be made. First, injection-induced and natural swarms follow the same scaling $V \propto T^{-\gamma}$, with $\gamma \sim 0.6$ and $\gamma \sim 0.7$, respectively. The continuous scaling of velocity with duration for all swarms is direct evidence that both types of sequences, natural and injection-induced, obey the same physics for all velocity ranges (from a few meters per day in the Ubaye and Cahuilla years-long sequences, to $\sim 1,100$ m/day for Rittershoffen which barely lasts a day). As anthropogenic seismicity is induced (though indirectly) by fluid injection (Bentz et al., 2020), this similar scaling suggests that natural swarms studied here are also a consequence of fluid pressure perturbations.

As expected the velocity–duration scaling of SSEs does not align with that of fluid-induced swarms, as they show 2 orders of magnitude higher migration velocities for a given duration, typically around 1–10 km/day (Gao et al., 2012). Interestingly, the velocity and duration of the Salton Trough earthquake swarm (Lohman & McGuire, 2007) lie close to those of SSEs. This is not surprising given that this swarm is thought to be purely driven by aseismic slip (Roland & McGuire, 2009), characterized by high migration velocities (2–3 orders of magnitude above the usual values), without an identified fluid trigger. This example shows that based on velocity and duration values, it is possible to differentiate swarms driven directly by fluid-induced aseismic slip (blue points—Figure 4) from slow-slip-driven swarms. The latter can be attributed to creep (Lohman & McGuire, 2007) or

to SSEs (Hirose et al., 2014), without requiring fluid injection. Velocity alone is not a sufficient discriminator: fluid-induced swarms with very short duration may have migration velocity higher than 1 km/day, a range of values that has been classically attributed to SSE (Lengline et al., 2017).

Moreover, the migration velocity obtained by numerical modeling of a fluid injection in a highly permeable, slip-weakening fault (Wynants-Morel et al., 2020) perfectly scales with the other fluid-induced swarms (Figure 4). This confirms that the model assumed in Figure 3, consistent with these numerical simulations, appears appropriate to explain the fluid-induced earthquake swarms with a possible prevalence of aseismic slip transients as trigger of seismic ruptures.

Despite the higher migration velocities of SSEs, the velocity–duration scaling is similar for swarms ($V \propto T^{-0.55}$) and SSEs ($V \propto T^{-0.5}$). The small difference of scaling exponents can be explained by different methods and uncertainties in the velocity measures for swarms and SSEs, and by the limited number of data points. The scaling similarity indicates that the migration of swarms may globally behave like the propagation of aseismic slip, supporting our assumption that $V_{\text{rupt}} = V_{\text{migr}}$. The observed scaling for swarms, $V \propto T^{-0.55}$, is compatible with fluid pressure diffusion. To explain this scaling within a diffusion framework, an average diffusivity of ~ 0.1 m²/s is needed. While such a value has been commonly inferred to explain earthquake swarm migration (e.g., Talwani & Acree, 1985), hydraulic diffusivities measured in laboratory or in field experiments are usually several order of magnitude lower (Doan et al., 2006). Also, a similar scaling is obtained for SSEs, which exhibit diverse migration shapes, often linear (Houston et al., 2011), and are not directly driven by fluid diffusion. Numerical modeling studies have demonstrated that individual SSEs migration can be explained by frictional process along rate-and-state faults without the need to include pore pressure diffusion as driving factor of seismicity (Li & Liu, 2016; Luo & Liu, 2019). Other mechanisms have been proposed to explain such scaling for SSEs, like a uniform stress drop or a uniform slip over the ruptured area, leading to exponents similar to the one observed Figure 4, of $-2/3$ or -0.5 , respectively (Ide et al., 2007). These mechanisms might also apply for swarms. Therefore, a general scaling compatible with diffusion does not imply that individual swarms are directly driven by

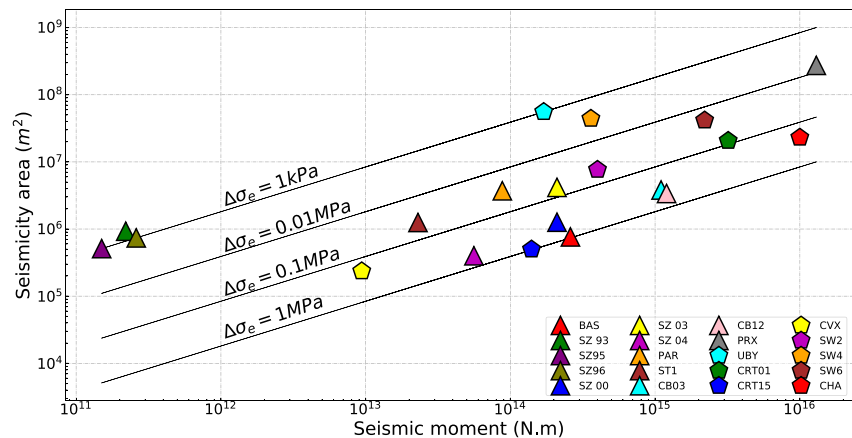


Figure 5. Seismicity area (m^2) as a function of the cumulative seismic moment during 20 of the swarms studied here (the two Rittershoffen swarms had no seismic moment available so they are not represented here). Triangles correspond to injection-induced sequences, while pentagons refer to natural swarms. Black lines represent different values of the effective stress drop $\Delta\sigma_e$.

fluid pressure diffusion. The similarity between SSE and swarm scaling suggests that swarm migration velocity may be globally consistent with an aseismic slip migration velocity.

The effective stress drop $\Delta\sigma_e$ for the swarms studied here is found to be comprised between 1 kPa and 1 MPa (Figure 5). Those values are lower than typical values of static stress drop for earthquakes, which usually range from 1 to 100 MPa (Cocco et al., 2016), and are more similar to the stress drop values estimated for SSEs (between 0.01 and 1 MPa; Brodsky & Mori, 2007; Gao et al., 2012). Thus, from this comparison, $\Delta\sigma_e$ values may indicate an aseismic component in the swarm processes. Given the similar values found for natural and injection-induced swarms, such an aseismic component would be ubiquitous to the swarms studied here. Indeed, following Fischer and Hainzl (2017), low values of $\Delta\sigma_e$ (between 0.01 and 1 MPa) suggest that seismic events are sparsely distributed over the active area, requiring an aseismic slip process to occur in between seismically slipping patches. Higher values of $\Delta\sigma_e$ for swarms could mean that seismic asperities are covering a large part of the seismicity area, and hence a smaller expected aseismic component compared to lower values of $\Delta\sigma_e$. Interestingly, variability can be observed in effective stress drop values. For instance, $\Delta\sigma_e \sim 1$ kPa for the Soultz-sous-Forêt stimulations (1993, 1995, and 1996) suggests an important aseismic moment release, while $\Delta\sigma_e = 1$ MPa for the Basel injection might mean that the contribution of aseismic slip is relatively less important in this case. Therefore, variability in effective stress drop values within the studied sequences might indicate variability in the importance of aseismic slip release among swarms, and $\Delta\sigma_e$ could be considered as a valuable proxy to the seismic-to-total moment ratio (Danré et al., 2022).

Based on similar velocity–duration scaling and effective stress drop values, natural and injection-induced swarms appear to share the same driving processes, in which aseismic slip seems ubiquitous, like depicted in Figure 3. The seismicity front delineates the aseismic slip rupture front and the seismicity area corresponds to the aseismic slip area, in a similar way as tremor locations in SSEs zones delineate slip migration and area (Bartlowet et al., 2011). However, as suggested by the variability of $\Delta\sigma_e$ values, the aseismic contribution might be different from one swarm to another.

4.2. Aseismic Contribution Differs Among Swarms

Based on the scaling of velocity versus duration for the studied swarms and their values of effective stress drop, it seems that aseismic slip is ubiquitous in those sequences. However, little is known about its quantitative importance in the moment budget of earthquake swarms, in part because of the observational limitations mentioned previously. To gain a better understanding, once the total moment $M_{0,\text{total}}$ for each swarm is computed (Equations 2 and 3), we compare it to the seismic moment using the seismic-to-total moment ratio r . A value of r close to 1 indicates that moment release is mainly seismic, while a low value shows that moment release is significantly aseismic. As shown in Figure 6a and Table S3 in Supporting Information S1, r ranges from 0.001 to almost 1. For

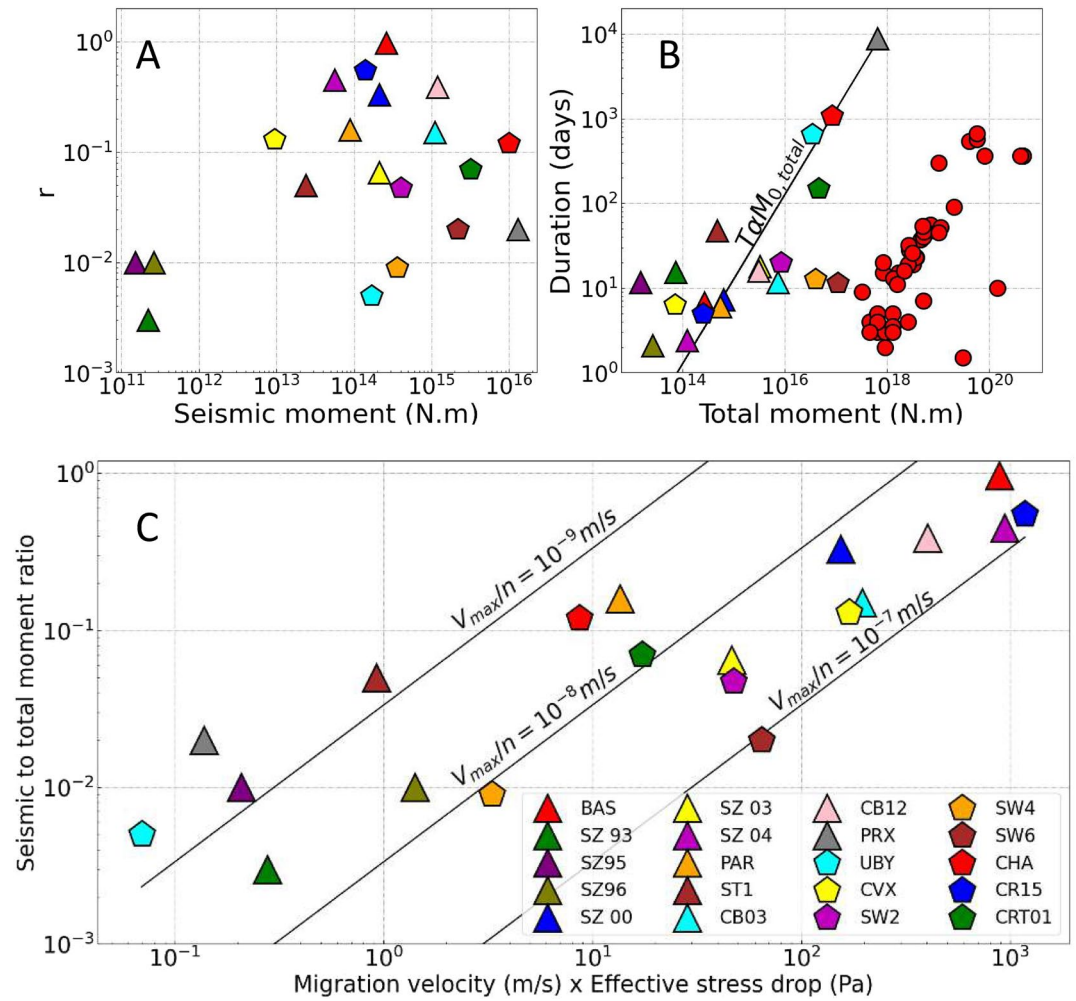


Figure 6. (a) Seismic-to-total moment ratio (r), as a function of the seismic moment released during each swarm, for the 20 sequences studied here. (b) Duration T as a function of the estimated total moment $M_{0,\text{total}}$. Black line represents the $\log(T) = \log(M_{0,\text{total}})$ line. Red dots correspond to the slow slip event (SSE) data from Gao et al. (2012). (c) Seismic-to-total moment ratio for the swarms studied here, as a function of the product of the migration velocity and the effective stress drop. The black lines correspond to different values of V_{max}/n , assuming $G = 30$ GPa (see Equation 8 and Figure S3 in Supporting Information S1 with $G = 15$ GPa).

the Basel injection-induced sequence, $r = 0.97$, suggesting that aseismic deformation is low in this case, while for the Ubaye natural swarm, $r = 0.005$, indicating aseismic moment release is dominant.

For the Soutz 1993 sequence, despite an injected fluid volume of the same order of magnitude as in the Basel injection (Deichmann & Giardini, 2009), the cumulative seismic moment is 3 orders of magnitude lower than the Basel one. This can be explained by the important aseismic moment release ($r \sim 0.001$) during the Soutz sequence. Therefore, our computations seem to validate that the strong difference of seismic moment release for similar injected volumes observed for injection-induced earthquake swarms can simply reflect the amount of induced aseismic deformation (De Barros, Cappa, et al., 2019; McGarr & Barbour, 2018).

Interestingly, we also observe that the slope of duration versus estimated total moment (Figure 6b) seems to be close to 1, similarly to the scaling between event duration and total moment observed for SSEs (Ide et al., 2007; Peng & Gomberg, 2010). This correlation is quite weak, but seismic moment versus duration does not exhibit such a scaling (Passarelli et al., 2018). Our total moment estimate accounts for the “hidden” aseismic slip release occurring during swarms. In the compilation of duration versus moment observations by Peng and Gomberg (2010), many swarms present much longer duration than SSEs, given similar moments. This difference can be explained

if the aseismic moment contribution in swarms, which has not been accounted for, is significant, leading to a scaling for swarms similar to the SSE one.

Based on the similarities observed between swarms and SSEs (Figures 4 and 6b), we apply the theoretical framework initially developed for SSEs to try to relate the seismic-to-total moment ratio to two observables, the effective stress drop and the migration velocity (Equation 8, see Figure 6c). We estimate V_{\max}/n being between 10^{-10} and 10^{-7} m/s, which corresponds to a maximum slip velocity V_{\max} consistent with expected orders of magnitudes (Glowacka et al., 2001; Roland & McGuire, 2009) if we consider a value of $n \sim 10$ (Hawthorne & Rubin, 2013; Lambert et al., 2021). Variability in V_{\max} explains why the observed scaling between r and $\Delta\sigma_e \times V_{\text{migr}}$ is not as linear as expected. As the general trend shows a scaling different than the isovalues of V_{\max}/n , it means that V_{\max} also depends, through fault and stress properties, on the seismic-to-total moment ratio.

5. Discussion and Conclusions

In addition to the numerous observations in the literature of similarities between natural and injection-induced earthquake swarms, our global analysis of both types of swarms helps to better understand their underlying processes. Indeed, based on the effective stress drop values and the velocity versus duration scaling similarity, the drivers of natural and anthropogenic swarms appear to be the same. For many years, swarms were thought to be solely driven by fluid pressure diffusion (Talwani & Acree, 1985). This has been proven to efficiently explain the migration of seismicity, assuming that the seismicity front is the fluid pressure front, and considering that the hydraulic diffusivity only varies in a narrow range (Talwani et al., 2007). Even if we cannot rule out a direct effect of the fluid pressure, we here show that a fluid-induced aseismic slip that triggers seismicity is also a suitable driving process for swarms at different scales. Indeed, considering aseismic slip helps to better explain some observations made on earthquake swarms, such as their global scaling of migration velocity versus duration being similar to that of SSEs (Figure 4) and their low effective stress drop values.

Furthermore, it appears that the role of aseismic slip is not limited to static slip but might be a key in explaining the dynamics of swarms. Indeed, through shear stress transfer at its tips, aseismic slip triggers a migrating seismicity (Figure 3). Such a stress transfer originating from an aseismic slip zone and seismicity triggering has been observed in different contexts like in the Boso Peninsula in Japan where two SSEs led to two earthquake swarms at their tips (Hirose et al., 2014), as well as in numerical modeling (Bhattacharya & Viesca, 2019; Wynants-Morel et al., 2020). The two different regimes observed in Figure 4, previously studied when comparing swarms on transform faults to their injection-induced counterparts (Roland & McGuire, 2009), for fluid-induced earthquake swarms and slow-slip-like transients in our case are separated by ~ 2 orders of magnitude in migration velocity. One could explain such a difference using Equation 5: a difference of ~ 2 orders of magnitude in stress drop for the two types of slip events would be consistent with the observed difference in migration velocity. Indeed, stress drop values reported for SSEs usually range from 0.01 to 0.1 MPa (Gao et al., 2012), which is 2 orders of magnitude smaller than our estimation of the total stress drop $\Delta\sigma_{\text{total}} = 7M_{0,\text{total}}/16R^3$ inferred from the total seismic moment for fluid-induced swarms, which are between 1 and 10 MPa. However, investigating the reasons behind such a difference in stress drop between fluid-induced swarms and SSEs is beyond the scope of this paper.

As mentioned above, our migration velocity measurements are based on average velocities, but some information might be left out. De Barros et al. (2021) indeed showed that seismic fronts have a complex time-dependent shape, revealing the seismogenic state of faults. However, we still get reliable results depicting the behavior of swarms, not on an individual but on a global scale.

If aseismic slip provides an explanation for the observations made on swarms, making parallels with existing aseismic transients gives more information on its importance. Using observations made on repeating earthquake sequences, we were able to compute total (and therefore aseismic) moment of swarms. While our quantification of total moment is rough and relies on several simplifying assumptions, we hope that further systematic study of relevant parameters like earthquake static stress drop, among others, will help confirm our findings. For instance, total moment estimation might be sensitive to parameters like the b -value from the Gutenberg-Richter law: a high b -value means that seismic energy is determined by an ensemble of small earthquakes in opposition with a low b -value for which a single earthquake is prominent. Our approach with D_{\max} might therefore be challenged for sequences with a high b -value, for which average slip might be better estimated by taking into account the

cumulative seismic slip, computed on a spatial grid for instance, rather than by only considering the biggest event. However, as a first approximation, the value obtained with D_{\max} seems to be a reasonable estimate of total moment released, as validated in another work (Danré et al., 2022).

Still, our results indicate that the importance of aseismic slip differs among swarms; even though it always drives seismicity, it can sometimes represent a small fraction of the deformation (like for the Basel case) or actually be the main slip mode (like for the Soultz 1993 sequence). While a seismicity migration governed by aseismic slip and a high seismic-to-total moment ratio, like for the Basel sequence, seem contradictory, this contradiction is only apparent: the former concerns only the seismicity front, while the latter involves the whole swarm, spatially and temporally. Aseismic slip might therefore play a key role in controlling earthquake migration through shear stress transfer (Figures 3 and 4), while seismicity behind the aseismic slip front might result from a combination of several processes including aseismic slip, interactions between earthquakes or fluid pressure triggering.

Our approach overcomes the difficulties caused by the low and long deformations occurring during those sequences, preventing geodetic observations in most cases. Aseismic slip in between the seismically slipping patches (Figure 3) would then explain the observed discrepancies between expected and observed seismic moment for fluid injections (McGarr & Barbour, 2018). The aseismic slip quantification proposed here is consistent, at first order, with the observed discrepancies. Based on the studies of SSEs, we introduced a simple mechanical model to relate different observables (Equation 8). This allows to give a physical sense to their measurements and provides a first-order physical approach to the slip dynamics during swarms. Further work on earthquake swarms might help identifying or better constraining the relevant parameters to model and understand in detail swarm dynamics.

Here, we also show that the slip velocity, together with the migration velocity and the effective stress drop, is the crucial parameters to characterize the seismic and aseismic moment partitioning in swarms. Among other properties, these three parameters depend on the stress state and on the proximity of the fault to failure (De Barros et al., 2021; Fischer & Hainzl, 2017; Hainzl & Fischer, 2002; Passelègue et al., 2020; Wynants-Morel et al., 2020). These relationships therefore deserve to be investigated in order to anticipate the swarm evolution, especially given that similarities are found between swarms and foreshock sequences of some major earthquakes (X. Chen & Shearer, 2013).

We here worked on catalogs selected for their simplicity (simple injection history and geometry) and discarded from the analysis swarms from different contexts (e.g., subduction, volcanoes). However, we have reconciled observations made since decades on the two types of swarms, injection-induced and natural, by proposing a realistic scenario involving fluid-induced aseismic slip triggering seismicity, based on multiple observations made on 22 sequences. This opens interesting perspectives to better understand seismic swarms, their propagation, and to improve their monitoring in order to anticipate potential large earthquakes. It also paves the way to study natural and injection-induced swarms as the same phenomena.

Data Availability Statement

Data for the Iceland swarms were kindly made available by the Icelandic Meteorological Office (SIL, <https://en.vedur.is/>) and L. Passarelli (Passarelli et al., 2018). Data from the Paralana sequence and from the Ubaye swarm were made available by J. Albaric (Albaric et al., 2014) and G. Daniel (Daniel et al., 2011), respectively. Catalog for the Cahuilla swarm were provided by Z. Ross and D. Trugman (Ross et al., 2020). Data for the Soultz fluid injections are available on the CDGP web services (<https://cdgp.u-strasbg.fr/>). Data for the Cooper Basin injections are available on the EPOS platform (<https://tcs.ah-epos.eu/>). Data for the Paradox Valley fluid injection are available on the US Bureau of Reclamation (<https://www.usbr.gov/uc/progact/paradox/index.html>). Rittershoffen data were made available by O. Lengliné (Lengliné et al., 2017). All data (earthquake swarms catalogs) used in this study can be retrieved through the data sources described in Table S3 in Supporting Information S1.

References

- Ake, J., Mahrer, K., O'Connell, D., & Block, L. (2005). Deep-injection and closely monitored induced seismicity at Paradox Valley, Colorado. *Bulletin of the Seismological Society of America*, 95(2), 664–683. <https://doi.org/10.1785/0120040072>
- Albaric, J., Oye, V., Langet, N., Hastings, M., Lecomte, I., Iranpour, K., et al. (2014). Monitoring of induced seismicity during the first geothermal reservoir stimulation at Paralana, Australia. *Geothermics*, 52, 120–131. <https://doi.org/10.1016/j.geothermics.2013.10.013>

Acknowledgments

We thank the editor Rachel Abercrombie and two anonymous reviewers whose comments helped improve this paper.

- Ampuero, J. P., & Rubin, A. M. (2008). Earthquake nucleation on rate and state faults—Aging and slip laws. *Journal of Geophysical Research*, *113*, B01302. <https://doi.org/10.1029/2007JB005082>
- Baisch, S., Rotherth, E., Stang, H., Vörös, R., Koch, C., & McMahon, A. (2015). Continued geothermal reservoir stimulation experiments in the Cooper Basin (Australia). *Bulletin of the Seismological Society of America*, *105*(1), 198–209. <https://doi.org/10.1785/0120140208>
- Baisch, S., Weidler, R., Vörös, R., Wyborn, D., & de Graaf, L. (2006). Induced seismicity during the stimulation of a geothermal HFR reservoir in the Cooper Basin, Australia. *Bulletin of the Seismological Society of America*, *96*(6), 2242–2256. <https://doi.org/10.1785/0120050255>
- Bartlow, N. M., Miyazaki, S., Bradley, A. M., & Segall, P. (2011). Space–time correlation of slip and tremor during the 2009 Cascadia slow slip event. *Geophysical Research Letters*, *38*, L18309. <https://doi.org/10.1029/2011GL048714>
- Bentz, S., Kwiatek, G., Martínez-Garzón, P., Bohnhoff, M., & Dresen, G. (2020). Seismic moment evolution during hydraulic stimulations. *Geophysical Research Letters*, *47*, e2019GL086185. <https://doi.org/10.1029/2019GL086185>
- Bhattacharya, P., & Viesca, R. C. (2019). Fluid-induced aseismic fault slip outpaces pore-fluid migration. *Science*, *364*(6439), 464–468. <https://doi.org/10.1126/science.aaw7354>
- Bourouis, S., & Bernard, P. (2007). Evidence for coupled seismic and aseismic fault slip during water injection in the geothermal site of Soultz (France), and implications for seismogenic transients. *Geophysical Journal International*, *169*(2), 723–732. <https://doi.org/10.1111/j.1365-246x.2006.03325.x>
- Brodsky, E. E., & Mori, J. (2007). Creep events slip less than ordinary earthquakes. *Geophysical Research Letters*, *34*, L16309. <https://doi.org/10.1029/2007GL030917>
- Calò, M., & Dorbath, C. (2013). Different behaviours of the seismic velocity field at Soultz-sous-Forêts revealed by 4-D seismic tomography: Case study of GPK3 and GPK2 injection tests. *Geophysical Journal International*, *194*(2), 1119–1137. <https://doi.org/10.1093/gji/ggt153>
- Cappa, F., Scuderi, M. M., Collettini, C., Guglielmi, Y., & Avouac, J. P. (2019). Stabilization of fault slip by fluid injection in the laboratory and in situ. *Science Advances*, *5*(3), eaau4065. <https://doi.org/10.1126/sciadv.aau4065>
- Charléty, J., Cuenot, N., Dorbath, L., Dorbath, C., Haessler, H., & Frogneux, M. (2007). Large earthquakes during hydraulic stimulations at the geothermal site of Soultz-sous-Forêts. *International Journal of Rock Mechanics and Mining Sciences*, *44*(8), 1091–1105. <https://doi.org/10.1016/j.ijrmms.2007.06.003>
- Chen, T., & Lapusta, N. (2009). Scaling of small repeating earthquakes explained by interaction of seismic and aseismic slip in a rate and state fault model. *Journal of Geophysical Research*, *114*, B01311. <https://doi.org/10.1029/2008JB005749>
- Chen, X., & Shearer, P. M. (2013). California foreshock sequences suggest aseismic triggering process. *Geophysical Research Letters*, *40*, 2602–2607. <https://doi.org/10.1002/grl.50444>
- Chen, X., Shearer, P. M., & Abercrombie, R. E. (2012). Spatial migration of earthquakes within seismic clusters in Southern California: Evidence for fluid diffusion. *Journal of Geophysical Research*, *117*, B04301. <https://doi.org/10.1029/2011JB008973>
- Cocco, M., Tinti, E., & Cirella, A. (2016). On the scale dependence of earthquake stress drop. *Journal of Seismology*, *20*(4), 1151–1170. <https://doi.org/10.1007/s10950-016-9594-4>
- Cuenot, N., Dorbath, C., & Dorbath, L. (2008). Analysis of the microseismicity induced by fluid injections at the EGS site of Soultz-sous-Forêts (Alsace, France): Implications for the characterization of the geothermal reservoir properties. *Pure and Applied Geophysics*, *165*(5), 797–828. <https://doi.org/10.1007/s00024-008-0335-7>
- Daniel, G., Prono, E., Renard, F., Thouvenot, F., Hainzl, S., Marsan, D., et al. (2011). Changes in effective stress during the 2003–2004 Ubaye seismic swarm, France. *Journal of Geophysical Research*, *116*, B01309. <https://doi.org/10.1029/2010JB007551>
- Danré, P., De Barros, L., & Cappa, F. (2022). Inferring fluid volume during earthquake swarms using seismic catalogues. *Geophysical Journal International*, *232*(2), 829–841. <https://doi.org/10.1093/gji/ggac345>
- De Barros, L., Baques, M., Godano, M., Helmstetter, A., Deschamps, A., Larroque, C., & Courboulex, F. (2019). Fluid-induced swarms and coseismic stress transfer: A dual process highlighted in the aftershock sequence of the 7 April 2014 earthquake (MI 4.8, Ubaye, France). *Journal of Geophysical Research: Solid Earth*, *124*(4), 3918–3932. <https://doi.org/10.1029/2018JB017226>
- De Barros, L., Cappa, F., Deschamps, A., & Dublanche, P. (2020). Imbricated aseismic slip and fluid diffusion drive a seismic swarm in the Corinth Gulf, Greece. *Geophysical Research Letters*, *47*, e2020GL087142. <https://doi.org/10.1029/2020GL087142>
- De Barros, L., Cappa, F., Guglielmi, Y., Duboeuf, L., & Grasso, J. R. (2019). Energy of injection-induced seismicity predicted from in-situ experiments. *Scientific Reports*, *9*(1), 1–11. <https://doi.org/10.1038/s41598-019-41306-x>
- De Barros, L., Wynants-Morel, N., Cappa, F., & Danré, P. (2021). Migration of fluid-induced seismicity reveals the seismogenic state of faults. *Journal of Geophysical Research: Solid Earth*, *126*, e2021JB022767. <https://doi.org/10.1029/2021JB022767>
- Deichmann, N., & Giardini, D. (2009). Earthquakes induced by the stimulation of an enhanced geothermal system below Basel (Switzerland). *Seismological Research Letters*, *80*(5), 784–798. <https://doi.org/10.1785/gssrl.80.5.784>
- Doan, M. L., Brodsky, E. E., Kano, Y., & Ma, K. F. (2006). In situ measurement of the hydraulic diffusivity of the active Chelungpu Fault, Taiwan. *Geophysical Research Letters*, *33*, L16317. <https://doi.org/10.1029/2006GL026889>
- Dublanche, P., & De Barros, L. (2021). Dual seismic migration velocities in seismic swarms. *Geophysical Research Letters*, *48*, e2020GL090025. <https://doi.org/10.1029/2020GL090025>
- Duboeuf, L. (2018). *Injections de fluide dans une zone de faille (LSBB, Rustrel): sismicité induite et déformation asismique* (Doctoral dissertation). Université Côte d'Azur.
- Duverger, C., Godano, M., Bernard, P., Lyon-Caen, H., & Lambotte, S. (2015). The 2003–2004 seismic swarm in the western Corinth rift: Evidence for a multiscale pore pressure diffusion process along a permeable fault system. *Geophysical Research Letters*, *42*, 7374–7382. <https://doi.org/10.1002/2015GL065298>
- Duverger, C., Lambotte, S., Bernard, P., Lyon-Caen, H., Deschamps, A., & Necessian, A. (2018). Dynamics of microseismicity and its relationship with the active structures in the western Corinth Rift (Greece). *Geophysical Journal International*, *215*(1), 196–221. <https://doi.org/10.1093/gji/ggy264>
- Dyer, B., Baria, R., & Michelet, S. (2004). *Soultz GPK3 stimulation and GPK3–GPK2 circulation May to July 2003—Seismic monitoring report* (Report no EEIG 05/2004). Semore Seismic for Socomine.
- Ellsworth, W. L. (2013). Injection-induced earthquakes. *Science*, *341*(6142), 1225942. <https://doi.org/10.1126/science.1225942>
- Eyre, T. S., Samsonov, S., Feng, W., Kao, H., & Eaton, D. W. (2022). InSAR data reveal that the largest hydraulic fracturing-induced earthquake in Canada, to date, is a slow-slip event. *Scientific Reports*, *12*(1), 1–12.
- Fischer, T., & Hainzl, S. (2017). Effective stress drop of earthquake clusters. *Bulletin of the Seismological Society of America*, *107*(5), 2247–2257. <https://doi.org/10.1785/0120170035>
- Fischer, T., & Hainzl, S. (2021). The growth of earthquake clusters. *Frontiers of Earth Science*, *9*, 79. <https://doi.org/10.3389/feart.2021.638336>
- Gao, H., Schmidt, D. A., & Weldon, R. J. (2012). Scaling relationships of source parameters for slow slip events. *Bulletin of the Seismological Society of America*, *102*(1), 352–360. <https://doi.org/10.1785/0120110096>

- Garagash, D. I. (2021). Fracture mechanics of rate-and-state faults and fluid injection induced slip. *Philosophical Transactions of the Royal Society A*, 379(2196), 20200129. <https://doi.org/10.1098/rsta.2020.0129>
- Gerard, A., Baumgärtner, J., Baria, R., & Jung, R. (1997). An attempt towards a conceptual model derived from 1993–1996 hydraulic operations at Soutz. In *Proceedings of NEDO International Symposium, Sendai, Japan* (Vol. 2, pp. 329–341).
- Glowacka, E., González, J. J., Nava, F. A., Farfan, F., & Diaz de Cossio, G. (2001). Monitoring surface deformations in the Mexicali valley, BC, Mexico. In *Proceedings of Tenth International Symposium on Deformation Measurements* (Vol. 175183).
- Goebel, T. H., & Brodsky, E. E. (2018). The spatial footprint of injection wells in a global compilation of induced earthquake sequences. *Science*, 361(6405), 899–904. <https://doi.org/10.1126/science.aat5449>
- Goebel, T. H., Hosseini, S. M., Cappa, F., Hauksson, E., Ampuero, J. P., Aminzadeh, F., & Saleeby, J. B. (2016). Wastewater disposal and earthquake swarm activity at the southern end of the Central Valley, California. *Geophysical Research Letters*, 43, 1092–1099. <https://doi.org/10.1002/2015GL066948>
- Goodfellow, S. D., Nasser, M. H. B., Maxwell, S. C., & Young, R. P. (2015). Hydraulic fracture energy budget: Insights from the laboratory. *Geophysical Research Letters*, 42, 3179–3187. <https://doi.org/10.1002/2015GL063093>
- Gualandi, A., Nichele, C., Serpelloni, E., Chiaraluce, L., Anderlini, L., Latorre, D., et al. (2017). Aseismic deformation associated with an earthquake swarm in the northern Apennines (Italy). *Geophysical Research Letters*, 44, 7706–7714. <https://doi.org/10.1002/2017GL073687>
- Guglielmi, Y., Cappa, F., Avouac, J. P., Henry, P., & Elsworth, D. (2015). Seismicity triggered by fluid injection–induced aseismic slip. *Science*, 348(6240), 1224–1226. <https://doi.org/10.1126/science.aab0476>
- Hainzl, S., & Fischer, T. (2002). Indications for a successively triggered rupture growth underlying the 2000 earthquake swarm in Vogtland/NW Bohemia. *Journal of Geophysical Research*, 107(B12), 2338. <https://doi.org/10.1029/2002JB001865>
- Hamiel, Y., Baer, G., Kalindefake, L., Dombola, K., & Chindandali, P. (2012). Seismic and aseismic slip evolution and deformation associated with the 2009–2010 northern Malawi earthquake swarm, East African Rift. *Geophysical Journal International*, 191(3), 898–908. <https://doi.org/10.1111/j.1365-246x.2012.05673.x>
- Hatch, R. L., Abercrombie, R. E., Ruhl, C. J., & Smith, K. D. (2020). Evidence of aseismic and fluid-driven processes in a small complex seismic swarm near Virginia City, Nevada. *Geophysical Research Letters*, 47, e2019GL085477. <https://doi.org/10.1029/2019GL085477>
- Hawthorne, J. C., & Rubin, A. M. (2013). Laterally propagating slow slip events in a rate and state friction model with a velocity-weakening to velocity-strengthening transition. *Journal of Geophysical Research: Solid Earth*, 118, 3785–3808. <https://doi.org/10.1002/jgrb.50261>
- Hensch, M., Riedel, C., Reinhardt, J., Dahm, T., & The NICE-People. (2008). Hypocenter migration of fluid-induced earthquake swarms in the Tjörnes Fracture Zone (North Iceland). *Tectonophysics*, 447(1–4), 80–94. <https://doi.org/10.1016/j.tecto.2006.07.015>
- Hirose, H., Matsuzawa, T., Kimura, T., & Kimura, H. (2014). The Boso slow slip events in 2007 and 2011 as a driving process for the accompanying earthquake swarm. *Geophysical Research Letters*, 41, 2778–2785. <https://doi.org/10.1002/2014GL059791>
- Holtkamp, S. G., & Brudzinski, M. R. (2011). Earthquake swarms in circum-Pacific subduction zones. *Earth and Planetary Science Letters*, 305(1–2), 215–225. <https://doi.org/10.1016/j.epsl.2011.03.004>
- Hoskins, M. C., Meltzer, A., Font, Y., Agurto-Detzel, H., Vaca, S., Rolandone, F., et al. (2021). Triggered crustal earthquake swarm across subduction segment boundary after the 2016 Pedernales, Ecuador megathrust earthquake. *Earth and Planetary Science Letters*, 553, 116620. <https://doi.org/10.1016/j.epsl.2020.116620>
- Houston, H., Delbridge, B. G., Wech, A. G., & Creager, K. C. (2011). Rapid tremor reversals in Cascadia generated by a weakened plate interface. *Nature Geoscience*, 4(6), 404–409. <https://doi.org/10.1038/ngeo1157>
- Ide, S., Beroza, G. C., Shelly, D. R., & Uchide, T. (2007). A scaling law for slow earthquakes. *Nature*, 447(7140), 76–79. <https://doi.org/10.1038/nature05780>
- Ito, Y., Obara, K., Shiomi, K., Sekine, S., & Hirose, H. (2007). Slow earthquakes coincident with episodic tremors and slow slip events. *Science*, 315(5811), 503–506. <https://doi.org/10.1126/science.1134454>
- Jenatton, L., Guiguet, R., Thouvenot, F., & Daix, N. (2007). The 16,000-event 2003–2004 earthquake swarm in Ubaye (French Alps). *Journal of Geophysical Research*, 112, B11304. <https://doi.org/10.1029/2006JB004878>
- Jiang, Y., Samsonov, S. V., & González, P. J. (2022). Aseismic fault slip during a shallow normal-faulting seismic swarm constrained using a physically-informed geodetic inversion method. *Journal of Geophysical Research: Solid Earth*, 127, e2021JB022621. <https://doi.org/10.1029/2021JB022621>
- Keranen, K. M., Savage, H. M., Abers, G. A., & Cochran, E. S. (2013). Potentially induced earthquakes in Oklahoma, USA: Links between wastewater injection and the 2011 Mw 5.7 earthquake sequence. *Geology*, 41(6), 699–702. <https://doi.org/10.1130/g34045.1>
- Keranen, K. M., & Weingarten, M. (2018). Induced seismicity. *Annual Review of Earth and Planetary Sciences*, 46(1), 149–174. <https://doi.org/10.1146/annurev-earth-082517-010054>
- Kim, W. Y. (2013). Induced seismicity associated with fluid injection into a deep well in Youngstown, Ohio. *Journal of Geophysical Research: Solid Earth*, 118, 3506–3518. <https://doi.org/10.1002/jgrb.50247>
- Kraft, T., Wassermann, J., Schmedes, E., & Igel, H. (2006). Meteorological triggering of earthquake swarms at Mt. Hochstaufen, SE-Germany. *Tectonophysics*, 424(3–4), 245–258. <https://doi.org/10.1016/j.tecto.2006.03.044>
- Kwiatk, G., Saarno, T., Ader, T., Bluemle, F., Bohnhoff, M., Chendorain, M., et al. (2019). Controlling fluid-induced seismicity during a 6.1-km-deep geothermal stimulation in Finland. *Science Advances*, 5(5), eaav7224. <https://doi.org/10.1126/sciadv.aav7224>
- Lambert, V., Lapusta, N., & Faulkner, D. (2021). Scale dependence of earthquake rupture prestress in models with enhanced weakening: Implications for event statistics and inferences of fault stress. *Journal of Geophysical Research: Solid Earth*, 126(10), e2021JB021886.
- Larochelle, S., Lapusta, N., Ampuero, J. P., & Cappa, F. (2021). Constraining fault friction and stability with fluid-injection field experiments. *Geophysical Research Letters*, 48, e2020GL091188. <https://doi.org/10.1029/2020GL091188>
- Lengliné, O., Boubacar, M., & Schmittbuhl, J. (2017). Seismicity related to the hydraulic stimulation of GRT1, Rittershoffen, France. *Geophysical Journal International*, 208(3), 1704–1715. <https://doi.org/10.1093/gji/ggw490>
- Lengliné, O., Lamourette, L., Vivin, L., Cuenot, N., & Schmittbuhl, J. (2014). Fluid-induced earthquakes with variable stress drop. *Journal of Geophysical Research: Solid Earth*, 119, 8900–8913. <https://doi.org/10.1002/2014JB011282>
- Li, D., & Liu, Y. (2016). Spatiotemporal evolution of slow slip events in a nonplanar fault model for northern Cascadia subduction zone. *Journal of Geophysical Research: Solid Earth*, 121, 6828–6845. <https://doi.org/10.1002/2016JB012857>
- Lohman, R. B., & McGuire, J. J. (2007). Earthquake swarms driven by aseismic creep in the Salton Trough, California. *Journal of Geophysical Research*, 112, B04405. <https://doi.org/10.1029/2006JB004596>
- Luo, Y., & Liu, Z. (2019). Rate-and-state model casts new insight into episodic tremor and slow-slip variability in Cascadia. *Geophysical Research Letters*, 46, 6352–6362. <https://doi.org/10.1029/2019GL082694>
- Madariaga, R. (1976). Dynamics of an expanding circular fault. *Bulletin of the Seismological Society of America*, 66(3), 639–666. <https://doi.org/10.1785/bssa0660030639>

- Matsuzawa, T., Uchida, N., Igarashi, T., Okada, T., & Hasegawa, A. (2004). Repeating earthquakes and quasi-static slip on the plate boundary east off northern Honshu, Japan. *Earth Planets and Space*, 56(8), 803–811. <https://doi.org/10.1186/bf03353087>
- McGarr, A. (2014). Maximum magnitude earthquakes induced by fluid injection. *Journal of Geophysical Research: Solid Earth*, 119, 1008–1019. <https://doi.org/10.1002/2013JB010597>
- McGarr, A., & Barbour, A. J. (2018). Injection-induced moment release can also be aseismic. *Geophysical Research Letters*, 45, 5344–5351. <https://doi.org/10.1029/2018GL078422>
- Metois, M., Vigny, C., & Socquet, A. (2016). Interseismic coupling, megathrust earthquakes and seismic swarms along the Chilean subduction zone (38–18°S). *Pure and Applied Geophysics*, 173(5), 1431–1449. <https://doi.org/10.1007/s00024-016-1280-5>
- Michellini, A., & Bolt, B. A. (1986). Application of the principal parameters method to the 1983 Coalinga, California, aftershock sequence. *Bulletin of the Seismological Society of America*, 76(2), 409–420. <https://doi.org/10.1785/bssa0760020409>
- Montgomery-Brown, E. K., Shelly, D. R., & Hsieh, P. A. (2019). Snowmelt-triggered earthquake swarms at the margin of Long Valley Caldera, California. *Geophysical Research Letters*, 46, 3698–3705. <https://doi.org/10.1029/2019GL082254>
- Parotidis, M., Shapiro, S. A., & Rothert, E. (2004). Back front of seismicity induced after termination of borehole fluid injection. *Geophysical Research Letters*, 31, L02612. <https://doi.org/10.1029/2003GL018987>
- Passarelli, L., Rivalta, E., Jónsson, S., Hensch, M., Metzger, S., Jakobsdóttir, S. S., et al. (2018). Scaling and spatial complementarity of tectonic earthquake swarms. *Earth and Planetary Science Letters*, 482, 62–70. <https://doi.org/10.1016/j.epsl.2017.10.052>
- Passelègue, F. X., Almakari, M., Dublanche, P., Barras, F., Fortin, J., & Violay, M. (2020). Initial effective stress controls the nature of earthquakes. *Nature Communications*, 11(1), 1–8. <https://doi.org/10.1038/s41467-020-18937-0>
- Peng, Z., & Gombert, J. (2010). An integrated perspective of the continuum between earthquakes and slow-slip phenomena. *Nature Geoscience*, 3(9), 599–607. <https://doi.org/10.1038/ngeo940>
- Raleigh, C. B., Healy, J. H., & Bredehoeft, J. D. (1976). An experiment in earthquake control at Rangely, Colorado. *Science*, 191(4233), 1230–1237. <https://doi.org/10.1126/science.191.4233.1230>
- Roland, E., & McGuire, J. J. (2009). Earthquake swarms on transform faults. *Geophysical Journal International*, 178(3), 1677–1690. <https://doi.org/10.1111/j.1365-246x.2009.04214.x>
- Roman, D. C., & Cashman, K. V. (2006). The origin of volcano-tectonic earthquake swarms. *Geology*, 34(6), 457–460. <https://doi.org/10.1130/g22269.1>
- Ross, Z. E., & Cochran, E. S. (2021). Evidence for latent crustal fluid injection transients in Southern California from long-duration earthquake swarms. *Geophysical Research Letters*, 48, e2021GL092465. <https://doi.org/10.1029/2021GL092465>
- Ross, Z. E., Cochran, E. S., Trugman, D. T., & Smith, J. D. (2020). 3D fault architecture controls the dynamism of earthquake swarms. *Science*, 368(6497), 1357–1361. <https://doi.org/10.1126/science.abb0779>
- Rubin, A. M. (2008). Episodic slow slip events and rate-and-state friction. *Journal of Geophysical Research*, 113, B11414. <https://doi.org/10.1029/2008JB005642>
- Ruhl, C. J., Abercrombie, R. E., Smith, K. D., & Zaliapin, I. (2016). Complex spatiotemporal evolution of the 2008 Mw 4.9 Mogul earthquake swarm (Reno, Nevada): Interplay of fluid and faulting. *Journal of Geophysical Research: Solid Earth*, 121, 8196–8216. <https://doi.org/10.1002/2016JB013399>
- Sáez, A., Lecampion, B., Bhattacharya, P., & Viesca, R. C. (2022). Three-dimensional fluid-driven stable frictional ruptures. *Journal of the Mechanics and Physics of Solids*, 160, 104754. <https://doi.org/10.1016/j.jmps.2021.104754>
- Schmidt, D. A., & Gao, H. (2010). Source parameters and time-dependent slip distributions of slow slip events on the Cascadia subduction zone from 1998 to 2008. *Journal of Geophysical Research*, 115, B00A18. <https://doi.org/10.1029/2008JB006045>
- Schultz, R., Atkinson, G., Eaton, D. W., Gu, Y. J., & Kao, H. (2018). Hydraulic fracturing volume is associated with induced earthquake productivity in the Duvernay play. *Science*, 359(6373), 304–308. <https://doi.org/10.1126/science.aao0159>
- Scotti, O., & Cornet, F. H. (1994). In situ evidence for fluid-induced aseismic slip events along fault zones. In *International Journal of Rock Mechanics and Mining Sciences & Geomechanics Abstracts* (Vol. 31(4), pp. 347–358). Pergamon.
- Seeber, L., Armbruster, J. G., & Kim, W. Y. (2004). A fluid-injection-triggered earthquake sequence in Ashtabula, Ohio: Implications for seismogenesis in stable continental regions. *Bulletin of the Seismological Society of America*, 94(1), 76–87. <https://doi.org/10.1785/0120020091>
- Shapiro, S. A., Huenges, E., & Borm, G. (1997). Estimating the crust permeability from fluid-injection-induced seismic emission at the KTB site. *Geophysical Journal International*, 131(2), F15–F18. <https://doi.org/10.1111/j.1365-246x.1997.tb01215.x>
- Shelly, D. R., Hill, D. P., Massin, F., Farrell, J., Smith, R. B., & Taira, T. A. (2013). A fluid-driven earthquake swarm on the margin of the Yellowstone caldera. *Journal of Geophysical Research: Solid Earth*, 118, 4872–4886. <https://doi.org/10.1002/jgrb.50362>
- Skoumal, R. J., Brudzinski, M. R., & Currie, B. S. (2015). Distinguishing induced seismicity from natural seismicity in Ohio: Demonstrating the utility of waveform template matching. *Journal of Geophysical Research: Solid Earth*, 120, 6284–6296. <https://doi.org/10.1002/2015JB012265>
- Talwani, P., & Acree, S. (1985). Pore pressure diffusion and the mechanism of reservoir-induced seismicity. In *Earthquake prediction* (pp. 947–965). Birkhäuser.
- Talwani, P., Chen, L., & Galalut, K. (2007). Seismogenic permeability, k_p . *Journal of Geophysical Research*, 112, B07309. <https://doi.org/10.1029/2006JB004665>
- Uchida, N. (2019). Detection of repeating earthquakes and their application in characterizing slow fault slip. *Progress in Earth and Planetary Science*, 6(1), 1–21. <https://doi.org/10.1186/s40645-019-0284-z>
- Vallée, M., Nocquet, J. M., Battaglia, J., Font, Y., Segovia, M., Regnier, M., et al. (2013). Intense interface seismicity triggered by a shallow slow slip event in the Central Ecuador subduction zone. *Journal of Geophysical Research: Solid Earth*, 118, 2965–2981. <https://doi.org/10.1002/jgrb.50216>
- Wang, L., Kwiatek, G., Rybacki, E., Bohnhoff, M., & Dresen, G. (2020). Injection-induced seismic moment release and laboratory fault slip: Implications for fluid-induced seismicity. *Geophysical Research Letters*, 47, e2020GL089576. <https://doi.org/10.1029/2020GL089576>
- Wech, A. G., & Bartlow, N. M. (2014). Slip rate and tremor genesis in Cascadia. *Geophysical Research Letters*, 41, 392–398. <https://doi.org/10.1002/2013GL058607>
- Wei, S., Avouac, J. P., Hudnut, K. W., Donnellan, A., Parker, J. W., Graves, R. W., et al. (2015). The 2012 Brawley swarm triggered by injection-induced aseismic slip. *Earth and Planetary Science Letters*, 422, 115–125. <https://doi.org/10.1016/j.epsl.2015.03.054>
- Wynants-Morel, N., Cappa, F., De Barros, L., & Ampuero, J. P. (2020). Stress perturbation from aseismic slip drives the seismic front during fluid injection in a permeable fault. *Journal of Geophysical Research: Solid Earth*, 125, e2019JB019179. <https://doi.org/10.1029/2019JB019179>
- Yang, Y., & Dunham, E. M. (2021). Effect of porosity and permeability evolution on injection-induced aseismic slip. *Journal of Geophysical Research: Solid Earth*, 126, e2020JB021258. <https://doi.org/10.1029/2020JB021258>
- Yoshida, K., & Hasegawa, A. (2018). Sendai-Okura earthquake swarm induced by the 2011 Tohoku-Oki earthquake in the stress shadow of NE Japan: Detailed fault structure and hypocenter migration. *Tectonophysics*, 733, 132–147. <https://doi.org/10.1016/j.tecto.2017.12.031>

- Zhu, W., Allison, K. L., Dunham, E. M., & Yang, Y. (2020). Fault valving and pore pressure evolution in simulations of earthquake sequences and aseismic slip. *Nature Communications*, *11*(1), 1–11. <https://doi.org/10.1038/s41467-020-18598-z>
- Zoback, M. D., & Gorelick, S. M. (2012). Earthquake triggering and large-scale geologic storage of carbon dioxide. *Proceedings of the National Academy of Sciences of the United States of America*, *109*(26), 10164–10168. <https://doi.org/10.1073/pnas.1202473109>

References From the Supporting Information

- Edwards, B., & Douglas, J. (2014). Magnitude scaling of induced earthquakes. *Geothermics*, *52*, 132–139. <https://doi.org/10.1016/j.geothermics.2013.09.012>
- Goertz-Allmann, B. P., Goertz, A., & Wiemer, S. (2011). Stress drop variations of induced earthquakes at the Basel geothermal site. *Geophysical Research Letters*, *38*, L09308. <https://doi.org/10.1029/2011GL047498>
- Hawthorne, J. C., Ampuero, J. P., & Simons, M. (2017). A method for calibration of the local magnitude scale based on relative spectral amplitudes, and application to the San Juan Bautista, California, area. *Bulletin of the Seismological Society of America*, *107*(1), 85–96. <https://doi.org/10.1785/0120160141>
- Herrmann, M., Kraft, T., Tormann, T., Scarabello, L., & Wiemer, S. (2019). A consistent high-resolution catalog of induced seismicity in Basel based on matched filter detection and tailored post-processing. *Journal of Geophysical Research: Solid Earth*, *124*, 8449–8477. <https://doi.org/10.1029/2019JB017468>
- Yeck, W. L., Block, L. V., Wood, C. K., & King, V. M. (2015). Maximum magnitude estimations of induced earthquakes at Paradox Valley, Colorado, from cumulative injection volume and geometry of seismicity clusters. *Geophysical Journal International*, *200*(1), 322–336. <https://doi.org/10.1093/gji/ggu394>